Available online at www.sciencedirect.com

ScienceDirect

www.elsevier.com/locate/jes

JES JOURNAL OF ENVIRONMENTAL SCIENCES

www.jesc.ac.cn

Effect of TiO_2 nanoparticle aggregation on marine microalgae *Isochrysis galbana*

Ji Hu[1], *Jianmin Wang*[2,*], *Shuxia Liu*[3], *Zhechao Zhang*[1], *Haifeng Zhang*[1], *Xiaoxia Cai*[1], *Jianming Pan*[1], *Jingjing Liu*[1]

1. *The Second Institute of Oceanography, State Oceanic Administration, Laboratory of Ecosystem and Biogeochemistry, State Oceanic Administration, Hangzhou 310012, China. E-mail: huj@sio.org.cn*
2. *Department of Civil, Architectural and Environmental Engineering, Missouri University of Science and Technology, Rolla, MO 65409, USA*
3. *Ocean College, Zhejiang University, Zhoushan 316021, China*

ARTICLE INFO

Article history:
Received 7 March 2017
Revised 13 May 2017
Accepted 16 May 2017
Available online 25 May 2017

Keywords:
Titanium dioxide
Nanoparticles
Aggregation
Marine microalgae
Ecotoxicity

ABSTRACT

TiO_2 nanoparticles (NPs) could adversely impact aquatic ecosystems. However, the aggregation of these NPs could attenuate this effect. In this work, the biological effects of TiO_2 NPs on a marine microalgae *Isochrysis galbana* were investigated. The aggregation kinetics of TiO_2 NPs under different conditions was also investigated to determine and understand these effects. Results showed that, though TiO_2 NPs had no obvious impact on the size and reproducibility of algal cells under testing conditions, they caused a negative effect on algal chlorophyll, which led to a reduction in photosynthesis. Furthermore, fast aggregation of TiO_2 NPs occurred under all conditions, especially at the pH close to the pH_{zpc}. Increasing ionic strength and NP concentration also enhanced the aggregation rate. The aggregation and the following sedimentation of TiO_2 NPs reduced their adverse effects on *I. galbana*.

Introduction

Nanoparticles (NPs) display unique physical and chemical characteristics such as large specific surface areas and unique surface structures that cause high surface reactivity. They are increasingly used for industrial and commercial purposes as catalysts, semiconductors, cosmetics, microelectronics, drug carriers, *etc*. The production of engineered NPs is expected to be 58,000 tons in 2020 (Mayland, 2006). The wide application of NPs has increased significant concerns about their environmental release and their potential toxicity to aquatic organisms such as marine phytoplankton (Miao et al., 2010; Matranga and Corsi, 2012; Miller et al., 2012).

TiO_2 NPs have been widely used in many commercial products (including self-cleaning and antimicrobial coatings/paintings, cosmetics, and sunscreens) because of their high chemical reactivity and broad UV attenuation properties (Maier, 2005; Chen, 2007). The direct release of TiO_2 NPs from urban applications to an aquatic system could achieve concentrations in μg/L (Kaegi, 2008). TiO_2 NPs can produce reactive oxygen species (ROS) which may induce oxidative damage to bacteria (Adams et al., 2006), fresh water invertebrate (Lovern and Klaper, 2006), and different cell types (Long et al., 2006; Rothen-Rutishauser et al., 2006).

The toxicity of NPs not only depends on their total concentration but also depends on their aggregate size and surface chemistry (Grassian, 2008; Gao et al., 2009). The size of aggregates was a key factor in determining their uptake and effect on cells (Rothen-Rutishauser et al., 2006), as well as their bioavailability to plant roots, algae, and fungi (Navarro

* *Corresponding author*. E-mail: wangjia@mst.edu (Jianmin Wang).

http://dx.doi.org/10.1016/j.jes.2017.05.026

et al., 2008a). Therefore, understanding the fate and transport of TiO_2 NPs in water was essential for determining their availability and toxicity on aquatic organisms.

Surface potential dominates the aggregation of NPs. In addition, pH, ionic strength, and cation valence affect the aggregation (Dunphy Guzman et al., 2006; French et al., 2009). Moreover, the presence of organic acid such as fulvic acid decreases TiO_2 NP aggregation (Domingos et al., 2009). The fastest aggregations were also observed at a pH close to the pH of zero point of charge (pH_{zpc}) under all conditions (Dunphy Guzman et al., 2006; Pettibone et al., 2008; Domingos et al., 2009; French et al., 2009).

Although the ecotoxicity of TiO_2 NPs in freshwater has been well studied, the effect of TiO_2 NPs on marine algae, a primary producer in marine ecosystem, has not been well understood. The objective of this research was to determine the effect of TiO_2 NPs on a marine microalgae, *Isochrysis galbana*. In addition, because the aggregation of NPs could significantly influence NP toxicity (Hotze et al., 2010), the aggregation kinetics of TiO_2 NPs were also investigated to develop insights into both the direct and indirect biological effects of NPs on a marine ecosystem. It was also important to assess the environmental risks related to the release of the NPs (Dale et al., 2015).

1. Materials and methods

1.1. NPs and chemicals

TiO_2 NPs were purchased from Skyspring Nanomaterials Inc. (USA), Product #: 7930DL. It had a purity of 99.9%, with an advertised main size of 5 nm. Its crystal was anatase, with a specific surface area greater than 150 m^2/g. Millipore water was produced by using a Synergy® ultrapure water system (Millipore, USA). NaOH (99%) and HNO_3 (67%) were purchased from Fisher Scientific (USA).

1.2. Preparation of NP suspension for toxicity tests

TiO_2 NP suspensions for toxicity tests were prepared by diluting a NP stock solution with Guillard f/2 culture medium (Guillard, 1975). The seawater of the f/2 culture medium was obtained from the Southern Ocean near Antarctica, with a sanity of 34‰, and then filtered through a 0.22 μm membrane filter and sterilized. The stock solution of TiO_2 NPs (1000 mg/L) was made by adding 0.1000 ± 0.001 g of TiO_2 NPs into 100 mL of the f/2 culture medium. This stock solution was sonicated for 10 min at 25 Hz in a water bath prior to use. Different volumes of this stock solution were added to the blank f/2 culture medium to create testing TiO_2 NP suspensions with concentrations of 0, 40, 100, 200, 400, 1000 mg/L, respectively. The toxicity test solution was prepared by mixing this testing TiO_2 NP suspensions with algae at a volume ratio of 1:1, so that the highest TiO_2 NP concentration in the toxicity test was 500 mg/L. While the environmentally relevant concentration of NPs was generally at μg/L level, the high concentration used in this research reflected a scenario when a concentrated waste stream was accidentally discharged into the near shore water in short-term. The change of pH for these TiO_2 NP suspensions during the experiment was less than 0.5 pH unit (from 7.55 to 8.01) during the experiment, meeting the organisation for economic co-operation and development (OECD) guideline for this type of experiment (OECD, 2011).

1.3. NP influence on algal growth and photosynthesis

I. galbana was provided by the Institute of Oceanology, Chinese Academy of Sciences (IOCAS, China). It was incubated using a f/2 culture medium in a lab several months prior to testing. Algae, with an initial cell density of 2.35×10^5 cells/mL, were used in all tests. The growth inhibition tests of *I. galbana* were conducted according to OECD guidelines for testing chemicals (OECD, 2011). Four milliliters of algal solution and 4 mL of TiO_2 NP suspension were transferred into each of the 17 × 100 mm polystyrene culture test tubes (Fisher, USA). All test tubes were then incubated at 24°C, under a light/dark ratio of 12 hr:12 hr, with an illumination of 4000 lx during the light on period. After 24, 48, 72, and 96 hr, the reference fluorescent units (RFUs) of the sample were detected by using a Trilogy fluorescent meter (Turner, USA). RFU represented a reference value of intravital chlorophyll, which indicated chlorophyll changes inside algae cells and could be used as an indicator of algal growth status. The culture medium and TiO_2 NP suspensions have different background RFUs, hence, the RFU of the sample was corrected by deducting the background RFU of the test tube from the total RFU. All tests were conducted in duplicate, and the culture tubes were shaken once at a time interval of 24 hr to re-suspend algae and NP aggregates.

A micro-respiration (MR) system (Unisense, Denmark) was employed to determine the photosynthesis of the samples after 96 hr of incubation. Samples were carefully transferred into a specially designed MR glass chamber (containing a stirrer) and then sealed with a special cap. The cap contained a hole through which the MR-oxygen sensor could be inserted into the chamber. The chamber volume was previously determined to be 2146 μL by using the method provided by the manufacturer. Then, the MR system (including its chamber, rack, stirrer, and oxygen sensor) was placed in a transparent Perspex water bath in an incubator, at a temperature of 24 ± 0.1°C, with a light intensity of 4000 lx. The oxygen concentration inside the MR chamber was measured and the photosynthesis was indicated by the rate of oxygen generation that was auto-calculated by the MicOx program. The cell density and size were measured using a Moxi Z mini automated cell counter (Orflo, USA).

1.4. Shading effect of TiO_2 NP suspensions

The TiO_2 NP suspension could physically block light and impact algae activity, even when there was no direct contact between them. In order to identify the effect of TiO_2 NPs on algae without any physical contact between them, a shading experiment was conducted. A test tube (with the same algae density as the algae control in a biological assay) was inserted in a customized 50 mL glass tube that contained 20 mL of 500 mg/L freshly prepared TiO_2 NP solution (resuspended every 24 hr). This was to avoid any contact by the algae with the NPs (illustrated in Fig. 1). The RFU, cell density and size, and the rate of oxygen generation of the algae, were measured after 96 hr. This test was also conducted in duplicate.

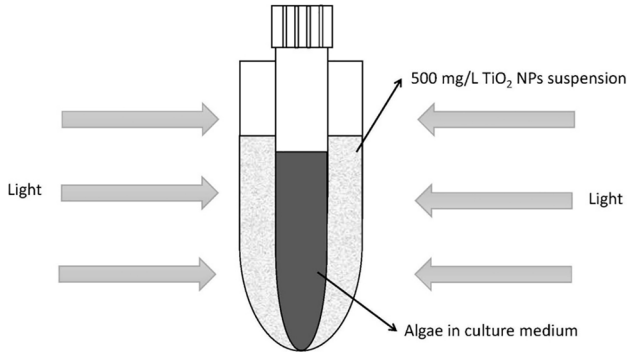

Fig. 1 – Diagram of shading effect of 500 mg/L TiO_2 nanoparticles on microalgae.

1.5. *Aggregation kinetics of TiO_2 NPs*

Nanosizer ZS-90 (Malvern Inc., UK) was used to measure zeta potential of TiO_2 NPs and their hydrodynamic diameters using a dynamic light scattering (DLS) method. Small quantities of TiO_2 NPs were added to MQ-water to obtain a 1000 mg/L stock solution. Samples of 100 μg/L to 100 mg/L were prepared by diluting the ultra-sonicated stock solution using an electrolyte solution with a certain pH and ionic strength. The sample pH finally ranged from 2 to 10, and the ionic strength ranged from 0.001 to 0.1 mol/L. In order to get low concentrations of TiO_2 NPs (such as 100 μg/L), secondary dilutions were made. A one-time intensive mixing was made following the dilution. After that, the sample was not mixed at all. Time zero was defined as the time of mixing. Data points were collected, with a certain time interval, until the hydrodynamic diameters had decreased or until no signals were observed because of the sedimentation of aggregates. This process usually took 20–30 min for 100 μg/L TiO_2 NPs, and longer for higher NP concentrations. The exact time was recorded by the instrument. All DLS analyses were carried out at 25°C, and all experiments were conducted in multiple replications.

If the aggregation was resulted from collisions by Brownian motion, the time-dependent decrease in the concentration of particles can be represented by a second-order rate law (Atkins and de Paula, 2005):

$$-\frac{dn}{dt} = kp \times n^2 \quad (1)$$

or

$$\frac{1}{n} - \frac{1}{n_o} = kp \times t \quad (2)$$

where n is the number concentration of NPs and kp is the aggregation constant. n can be expressed as

$$n = \frac{V_m}{V} = \frac{m}{\rho \times V} = \frac{3m}{\rho \times 4\pi R^3} \quad (3)$$

where m is the mass concentration of NPs, ρ is the density of aggregates, V_m is the total volume of aggregates per unit sorbent volume and V is the volume of a single aggregate, and R is the hydrodynamic radius of NPs (Phenrat et al., 2007).

By combining Eqs. (2) and (3), we can develop a quantitative expression of aggregate radius as a function of aggregation time:

$$R = \left(\frac{3m}{4\pi} \times \frac{kp}{\rho} \times t + {R_0}^3\right)^{1/3} \quad (4)$$

where R_0 is hydrodynamic radius of NPs at time zero.

ρ is difficult to determine. However, if we assume that the density of aggregates is a constant for TiO_2, a new constant Kp that is related to kp, $Kp = kp/\rho$, could be calculated based on Eq. (4) using a non-linear regression software. Kp can be used as an indicator of the aggregation rate to compare the aggregation of the same kind of NPs under different conditions.

1.6. *Data analysis*

A one-way analysis of variance (one-way ANOVA) was used to test the statistical significance of the toxicity results at 96 hr. A p value of less than 0.05 was considered statistically significant.

2. Results

2.1. *Influences of TiO_2 NPs on algal growth and photosynthesis*

Fig. 2 shows the algal growth indicated by algal RFU as a function of TiO_2 concentrations during the 24, 48, 72, and 96 hr culture period, respectively. It shows that, within the first 48 hr, the RFU decreased first and then increased with the increasing TiO_2 concentration. For example, at 24 hr, the RFU of algae with the 20 mg/L TiO_2 NPs decreased from 2960 ± 113 (control without NP) to 2118 ± 303 from the control (no NPs) of 2960 ± 113. However, the RFU increased slowly as greater NP concentrations were applied. Similarly, at 48 hr, the RFU with the 20 mg/L TiO_2 NPs decreased to 3549 ± 283 from the control of 4057 ± 22, then increased slowly as greater NP concentrations were applied. However, in the period of 72 hr to 96 hr, the algal RFU decreased with the increase of TiO_2 in the entire concentration range up to 500 mg/L TiO_2

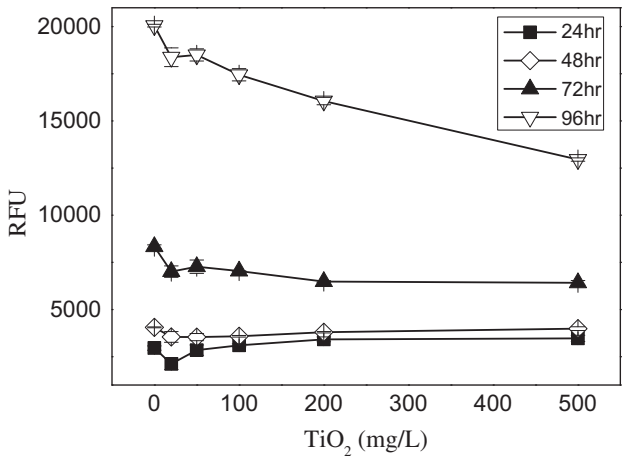

Fig. 2 – Influence of TiO_2 NPs on algae growth.

NPs, from 8344 ± 95 to 6420 ± 117 at 72 hr and 20,049 ± 71 to 12,951 ± 88 at 96 hr, respectively.

Table 1 depicts the algae RFU, density, size, and oxygen generation rate at 96 hr culturing period. It shows that the algal RFU decreased by 35% when the TiO_2 NP concentration increased from 0 to 500 mg/L ($p < 0.001$). Furthermore, there were no significant differences among algal sizes and algal density with different NP concentrations ($p > 0.05$) and almost no significant differences among algal sizes except for 50 mg/L TiO_2 NP. Similar to algal RFU, the oxygen generation rate, which exhibited a clear dose-dependent relationship, decreased from 463.3 ± 4.3 to 180.6 ± 5.8 nmol/hr (reduced by 61%) with the TiO_2 NP concentration increasing to 500 mg/L ($p < 0.001$).

2.2. Shading effect of TiO_2 NPs

Compared with algae control at 96 hr (Table 1), the algal RFU of the shaded sample decreased slightly to 17,997 ± 18 from the control of 20,049 ± 71 ($p = 0.011$), but no significant differences were found in algal density or algal size ($p > 0.05$). The oxygen generation rate under a shading effect of 500 mg/L TiO_2 NPs seemed a little lower than that of the control (459.7 ± 11.0 nmol/hr *vs.* 463.3 ± 4.3 nmol/hr), but no significant differences were identified in the statistics ($p > 0.05$). The relatively high standard deviation of the oxygen generation rate under shading effect may be responsible for the inconsistency between the RFU and the oxygen generation rate. Therefore, shading has a very minor impact on the growth of algae.

2.3. Impacts of pH, ionic strength, and NP concentration on NP aggregation

In order to better understand the effects of TiO_2 NPs on algal growth and photosynthesis, the aggregation kinetics of TiO_2 NPs were investigated under different pH, ionic strength, and NP concentration conditions. Eq. (4) was used to fit the aggregation data to determine the *Kp* value. Fig. 3 shows the *Kp* values for the 100 μg/L TiO_2 NP solution as a function of pH, under different ionic strength conditions. These 100 μg/L TiO_2 NP solutions were poly-dispersed throughout the aggregation process, with a Poly-Dispersion Index (PDI) of 1.0 for all measurements, according to Nanosizer's quality report. Poly-dispersion led to high standard deviations of hydrodynamic size measurement (French et al., 2009). However, the trends of these *Kp* values were very clear. They suggested that aggregation of TiO_2 NPs occurred over a wide range of pHs. The aggregation rate of TiO_2 NPs for all ionic strengths increased with the increase of pH before pH_{zpc} of approximately 5.5, which was determined based on a zeta potential measurement (Fig. 4). After reaching the maximum value at pH_{zpc}, the aggregation rate then decreased with the further increase in pH. The increased aggregation rate was consistent with the decrease in electrical repulsion. If the pH approached pH_{zpc}, the absolute value of the surface potential decreased, which caused less electrical repulsion.

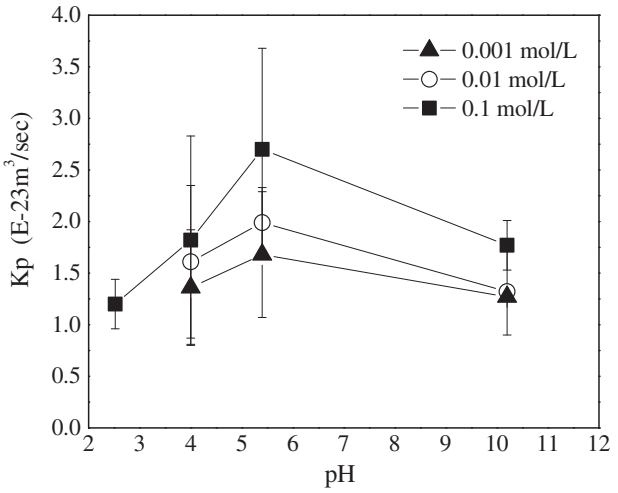

Fig. 3 – *Kp* as a function of pH at different ionic strengths with a TiO_2 NP concentration of 100 μg/L.

Fig. 3 shows that, under the ionic strength of 0.1 mol/L, the *Kp* at pH 10.3 was similar to that at pH 4, but greater than that at pH 2.4. According to Fig. 4, the zeta potential of TiO_2 NPs under an ionic strength of 0.1 mol/L at a pH of 10.3 was –19 mV, with an absolute value greater than that at pH conditions of 2.4 and 4.0, which were 12 mV and 3 mV, respectively. Based on the zeta potential value alone, the TiO_2 NPs aggregation rate at a pH of 10.3 should have been lower than those at the other two pH conditions. However, the actual *Kp* data have shown that, in addition to the zeta

Table 1 – Algal RFU, density, size, and oxygen generation rate at 96 hr.

TiO_2 (mg/L)	Algal fluorescence (RFU)	Algal density ($\times 10^6$ cells/mL)	Algal size (μm)	Oxygen generation rate (nmol/hr)
0	20,049 ± 71	2.12 ± 0.07	3.103 ± 0.005	463.3 ± 4.3
20	18,376 ± 496	1.92 ± 0.04	3.049 ± 0.020	436.0 ± 1.1
50	18,499 ± 325	2.14 ± 0.01	3.016 ± 0.002 *	429.9 ± 7.5 *
100	17,446 ± 325	1.99 ± 0.12	3.022 ± 0.012	375.4 ± 1.7 *
200	16,054 ± 196 *	1.97 ± 0.04	3.036 ± 0.004	313.2 ± 1.1 *
500	12,951 ± 88 *	1.89 ± 0.37	3.051 ± 0.031	180.6 ± 5.8 *
500 (shading effect)	17,997 ± 18 *	2.13 ± 0.02	3.102 ± 0.011	459.7 ± 11.0

RFU: reference fluorescent unit.

* Indicates the significance of difference ($p < 0.05$) between the control and the exposed treatments.

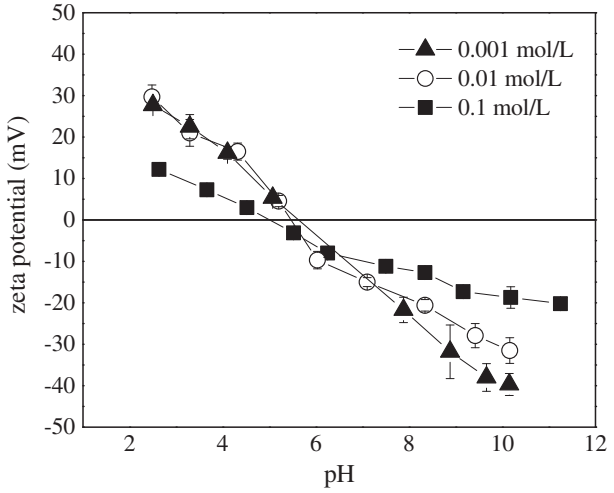

Fig. 4 – Zeta potentials of 100 μg/L TiO_2 NPs under different ionic strengths (0.001 mol/L, 0.01 mol/L, and 0.1 mol/L).

potential, the greater hydroxide concentration under a higher pH may have promoted the aggregation.

Fig. 3 also shows that increasing ionic strength increased the aggregation rate, due to the compression of the electrical double layer of the particles, as indicated by the decreased zeta potential (Fig. 4). These results were in agreement with previous publications (Domingos et al., 2009; French et al., 2009).

Fig. 5 shows aggregation data for different concentrations of NPs at an ionic strength of 0.001 mol/L. Within the first minute, hydrodynamic diameters of TiO_2 aggregates increased to 100, 400, 550, and 600 nm for TiO_2 NP concentrations of 0.1, 10, 50, and 100 mg/L, respectively. The increased NP concentration enhanced both the aggregation rate and the aggregate size, due to the increased collision among particles.

Although the experimental conditions used for the aggregation experiment were not exactly the same as those used for the toxicity experiment, the experimental data still provided fundamental information on the effect of TiO_2 NPs on *I. galbana*.

3. Discussion

The DLVO theory could be used to explain the aggregation mechanisms of TiO_2 NPs (Hotze et al., 2010). According to the DLVO theory, the interaction energy between two charged particles (*Vt*) in water is the sum of electrostatic double layer repulsion (*Vr*) and van der Waals attraction (*Va*). The following equations were used for total interaction energy calculation (Stumm and Morgan, 1981):

$$Vt = Vr + Va \tag{5}$$

$$Vr = \frac{64\pi rnkT\gamma^2}{\kappa^2} \times \exp(-\kappa H) \tag{6}$$

$$\gamma = \tanh\left(\frac{ze\varphi}{4kT}\right) \tag{7}$$

$$Va = -\frac{Ar}{12H} \tag{8}$$

$$Vt\ \max = \mathrm{MAX}(Vr + Va) \tag{9}$$

where *r* is the hydrodynamic radius of particle, κ^{-1} is the Debye screening length, *H* is the shortest interaction distance between two spherical particles, *k* is the Boltzmann constant, γ is the reduced surface potential, *n* is the number of ionic pairs in solvent, *T* is the absolute temperature, *z* is the valence of ion, *e* is the elementary charge, and φ is the surface potential (instead of which zeta potential was used as a very rough approximate here). The Hamaker constant, *A*, was proposed to the value of 5.53×10^{-20} J for TiO_2 in water (Bergström, 1997). The energy barrier (Vt_{max}) is usually characterized by the maximum net repulsion energy in a total interaction energy curve (Stumm and Morgan, 1981), and it can be calculated according Eqs. (5) to (9).

Increasing energy barrier led to increased stability of the particles. Fig. 6 shows the energy barrier as a function of pH for different ionic strengths. The energy barriers at pH 5.4 (for all ionic strengths) and those under an ionic strength of 0.1 mol/L (for all pH conditions) were negative. This meant

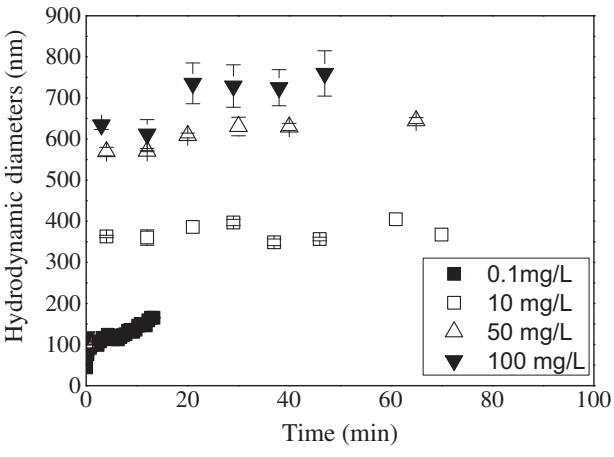

Fig. 5 – Aggregation kinetics of TiO_2 NPs with different NP concentrations at a pH of 5.4 and an ionic strength of 0.001 mol/L.

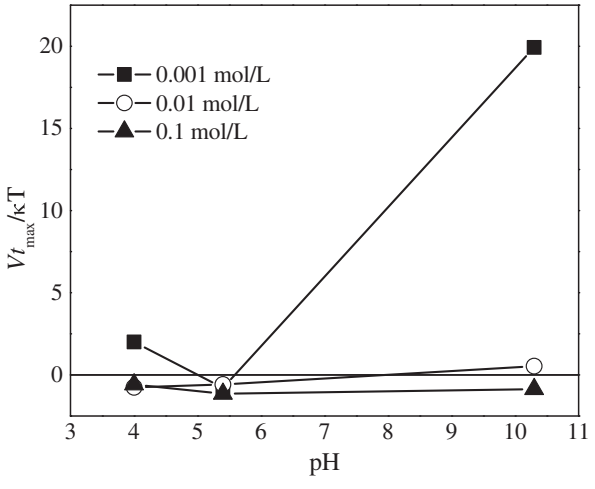

Fig. 6 – Total interaction energy as a function of pH under different ionic strengths (0.001 mol/L, 0.01 mol/L, and 0.1 mol/L). TiO_2 NP concentration was 100 μg/L.

that the electrical repulsion was less than the attraction. Therefore, it was relatively easy to form aggregates under these conditions. The lowest interaction energy barrier was found at a pH close to the pH_{zpc} under all ionic strengths. This was due to a low surface potential at this pH. Similar results were also found for other NPs, such as iron oxide (Baalousha, 2009). The energy barrier under an ionic strength of 0.001 mol/L and a pH of 10.3 was higher than the others, which indicated a relatively low aggregation rate. However, the real aggregation rate in the experiment under such conditions was not as low as expected. We speculated that a high concentration of hydroxide at a high pH may have promoted aggregation. Fig. 6 also shows that increasing ionic strength reduced the energy barrier. This was due to the decreased thickness of the diffuse electrical double layer, κ^{-1}, which led to decreased electrical repulsion. The DLVO theory was also successfully used to explain the ionic strength effect on the aggregation of other NPs, such as hematite NPs (He et al., 2008).

Aggregation of NPs could alter their effects on organisms by affecting ion release from the NP surfaces, size distribution and subsequent changes in biological uptake (Hotze et al., 2010), and exposure time and concentration resulted from deposition of large aggregates. Unlike silver NPs (Navarro et al., 2008b) and ZnO NPs (Miao et al., 2010; Ma et al., 2013), released ions from TiO_2 NPs were not the main reason for the toxicity (Lovern et al., 2007; Clément et al., 2013). Therefore, the effect of TiO_2 NPs in our tests could have come by two other pathways — the direct effect caused by the direct uptake and the indirect effect caused by the formation and deposition of large sized TiO_2 aggregates. According to our aggregation test, NPs quickly formed aggregates, and the size of aggregates significantly increased with the increase in NP concentration (Fig. 5). Although the aggregates may have had a direct toxic effect (Hund-Rinke et al., 2010), the formation of aggregates at least altered the exposure pathway and, therefore, indirectly impacted the toxicity.

The cell walls of the algae constituted a primary site and barrier for the entry of NPs into cells, and they typically contained glycoproteins and polysaccharides (Navarro et al., 2008a). Thus, only small NP aggregates could pass through the cell wall and reach the plasma membrane. However, the permeability of the cell wall could have changed during the reproduction period, and some large sized NP aggregates may have crossed the new synthesized cell walls (Ovečka et al., 2005). The marine algae *I. galbana* (used in this work) was naked, which means that NPs could directly reach the cell membrane (Calabrese and Davis, 1970). The lipid plasma membrane, which enclosed the cytoplasm, also restrained the entrance of NPs and NP aggregates (Fabrega et al., 2011). The endocytosis and phagocytosis promoted the cellular internalization of nanoscale (100 nm or less) and microscale (100–100,000 nm) NPs and NP aggregates, respectively (Moore, 2006). Combined with our aggregation data, a transition from endocytosis to phagocytosis with increases in exposure time or NP concentration was expected.

Furthermore, greater NP concentrations led to faster aggregation and larger aggregates. The increased size of aggregates enhanced their settling and, therefore, reduced suspended NP concentration. As shown in Appendix A Fig. S1, the absorbance of all NP suspensions decreased significantly in 6 hr, and the decrease was more significant with the increase in NP concentration (to lower than 10% with 500 mg/L TiO_2 NPs). This indicated a quick deposition. Hence, within the first 48 hr, the organisms had a similar exposure to NPs even with higher NP concentrations. When the test period was extended to 96 hr, the total exposure time of the organisms to TiO_2 NPs increased because of the resuspension of NPs every 24 hr. The adverse effect of TiO_2 NPs, which was probably caused by reactive oxygen species (ROS) (Miller et al., 2012), dominated the NP–organism interaction and, therefore, showed a clear dose-dependent relationship with algae. We recommend that aggregation or deposition tests of NPs should be conducted together with traditional ecotoxicity tests, so that the effect of NP aggregation on biological effects can be considered in lab or field tests.

TiO_2 NPs had low toxicity on algae growth under our test conditions, which were consistent with other research using marine phytoplankton (Miller et al., 2010). Although TiO_2 NPs had no obvious impact on the size and reproducibility of algal cells, they caused a negative effect on algal photosynthesis. TiO_2 aggregates may adsorb algae on the surface where TiO_2–algae complexes could participate in a ligand-to-metal charge transfer reaction (Carp et al., 2004), in which the algal cell wall is oxidized. Moreover, the ROS induced by TiO_2 NPs could damage cell membranes and inhibit photosynthesis (Lesser, 2006). Another process which may contribute to the reduction of algal fluorescence is quenching the emission intensity of chlorophyll *a* (Chl*a*) by NPs (Barazzouk et al., 2005; Falco et al., 2015; Queiroz et al., 2016). Appendix A Fig. S2 shows the impact of TiO_2 NPs (50 and 500 mg/L) on the fluorescence of Chl*a* chemical standards in acetone. The significant decrease in RFU of Chl*a* with 500 mg/L TiO_2 NPs after 96 hr of contact time indicated that TiO_2 NPs could also suppress the emission intensity of Chl*a*.

The results from the shading experiment indicated that a high TiO_2 NP concentration (500 mg/L) could block light to a certain degree and result in a negative impact on algal chlorophyll production. However, the shading effect of TiO_2 NPs contributed very slightly to its toxicity, even with a high NP concentration. It should be noted that the phototoxicity of TiO_2 NPs in our experiments may be underestimated by using artificial fluorescent light that emits very low ultraviolent, which could act as an antibacterial agent (Menard et al., 2011). Under natural light, ROS increased with increasing TiO_2 NP concentration, which may lead to an increase in overall toxicity (Miller et al., 2012).

4. Conclusions

The aggregation of TiO_2 NPs could directly impact the uptake of NPs by algae cells, and indirectly impact the exposure of algae cells to NPs by the deposition of NP aggregates. Therefore, increasing NP concentration may not proportionally increase the toxicity. TiO_2 NPs with a concentration of up to 500 mg/L exhibited an insignificant adverse effect on size and reproducibility, as well as a slight negative effect on the photosynthesis, of *I. galbana* algal cells. The fast aggregation of TiO_2 NPs should be taken into account when evaluating the toxicity of NPs.

Acknowledgments

This research was supported by the China Scholarship Council through a State-Sponsored Scholarship Program, NSF of China (No. 21307019), the Public Science and Technology Research Fund Projects of Ocean (No. 201505034), the Zhejiang Provincial Natural Science Foundation (Nos. LY14D060007 and LQ16D060006), and National Key Research and Development Program (No. 2016YFC1402405). The authors gratefully acknowledge the support from the Environment Research Center (ERC) at the Missouri University of Science and Technology, Rolla, Missouri, USA.

Appendix A. Supplementary data

Supplementary data to this article can be found online at http://dx.doi.org/10.1016/j.jes.2017.05.026.

REFERENCES

Adams, L.K., Lyon, D.Y., Alvarez, P.J.J., 2006. Comparative eco-toxicity of nanoscale TiO_2, SiO_2, and ZnO water suspensions. Water Res. 40 (19), 3527–3532.

Atkins, P., de Paula, J., 2005. Elements of Physical Chemistry. Oxford University Press, Oxford.

Baalousha, M., 2009. Aggregation and disaggregation of iron oxide nanoparticles: influence of particle concentration, pH and natural organic matter. Sci. Total Environ. 407 (6), 2093–2101.

Barazzouk, S., Kamat, P.V., Hotchandani, S., 2005. Photoinduced electron transfer between chlorophyll A and gold nanoparticles. J. Phys. Chem. B 109 (2), 716–723.

Bergström, L., 1997. Hamaker constants of inorganic materials. Adv. Colloid Interf. Sci. 70, 125–169.

Calabrese, A., Davis, H.C., 1970. Tolerances and requirements of embryos and larvae of bivalve molluscs. Helgoländer Meeresun. 20 (1), 553–564.

Carp, O., Huisman, C.L., Reller, A., 2004. Photoinduced reactivity of titanium dioxide. Prog. Solid State Chem. 32 (1), 33–177.

Chen, X., 2007. Titianium dioxide nanomaterials: synthesis, properties, modifications, and applications. Chem. Rev. 107, 2891–2959.

Clément, L., Hurel, C., Marmier, N., 2013. Toxicity of TiO_2 nanoparticles to cladocerans, algae, rotifers and plants — effects of size and crystalline structure. Chemosphere 90 (3), 1083–1090.

Dale, A.L., Casman, E.A., Lowry, G.V., Lead, J.R., Viparelli, E., Baalousha, M., 2015. Modeling nanomaterial environmental fate in aquatic systems. Environ. Sci. Technol. 49 (5), 2587–2593.

Domingos, R.F., Tufenkji, N., Wilkinson, K.J., 2009. Aggregation of titanium dioxide nanoparticles: role of a fulvic acid. Environ. Sci. Technol. 43 (5), 1282–1286.

Dunphy Guzman, K.A., Finnegan, M.P., Banfield, J.F., 2006. Influence of surface potential on aggregation and transport of titania nanoparticles. Environ. Sci. Technol. 40 (24), 7688–7693.

Fabrega, J., Luoma, S.N., Tyler, C.R., Galloway, T.S., Lead, J.R., 2011. Silver nanoparticles: behaviour and effects in the aquatic environment. Environ. Int. 37, 517–531.

Falco, W.F., Queiroz, A.M., Fernandes, J., Botero, E.R., Falcão, E.A., Guimarães, F.E.G., et al., 2015. Interaction between chlorophyll and silver nanoparticles: a close analysis of chlorophyll fluorescence quenching. J. Photochem. Photobiol. A Chem. 299, 203–209.

French, R.A., Jacobson, A.R., Kim, B., Isley, S.L., Penn, R.L., Baveye, P.C., 2009. Influence of ionic strength, pH, and cation valence on aggregation kinetics of titanium dioxide nanoparticles. Environ. Sci. Technol. 43 (5), 1354–1359.

Gao, J., Youn, S., Hovsepyan, A., Llaneza, V.n.L., Wang, Y., Bitton, G., et al., 2009. Dispersion and toxicity of selected manufactured nanomaterials in natural river water samples: effects of water chemical composition. Environ. Sci. Technol. 43 (9), 3322–3328.

Grassian, V.H., 2008. When size really matters: size-dependent properties and surface chemistry of metal and metal oxide nanoparticles in gas and liquid phase environments. J. Phys. Chem. C 112, 18308–18313.

Guillard, R.R.L., 1975. Culture of phytoplankton for feeding marine invertebrates. In: Smith, W.L., Chanley, M.H. (Eds.), Culture of Marine Invertebrate Animals: Proceedings — 1st Conference on Culture of Marine Invertebrate Animals Greenport. Springer US, Boston, MA, pp. 29–60.

He, Y., Wan, J., Tokunaga, T., 2008. Kinetic stability of hematite nanoparticles: the effect of particle sizes. J. Nanopart. Res. 10 (2), 321–332.

Hotze, E.M., Phenrat, T., Lowry, G.V., 2010. Nanoparticle aggregation: challenges to understanding transport and reactivity in the environment. J. Environ. Qual. 39 (6), 1909–1924.

Hund-Rinke, K., Schlich, K., Wenzel, A., 2010. TiO_2 nanoparticles — relationship between dispersion preparation method and ecotoxicity in the algal growth test. Umweltwiss. Schadst. Forsch. 22 (5), 517–528.

Kaegi, R., 2008. Synthetic TiO_2 nanoparticle emission from exterior facade into the aquatic environment. Environ. Pollut. 156, 233–239.

Lesser, M.P., 2006. Oxidative stress in marine environments: biochemistry and physiological ecology. Annu. Rev. Physiol. 68 (1), 253–278.

Long, T.C., Saleh, N., Tilton, R.D., Lowry, G.V., Veronesi, B., 2006. Titanium dioxide (P25) produces reactive oxygen species in immortalized brain microglia (BV2): implications for nanoparticle neurotoxicity. Environ. Sci. Technol. 40 (14), 4346–4352.

Lovern, S.B., Klaper, R., 2006. *Daphnia magna* mortality when exposed to titanium dioxide and fullerene (C_{60}) nanoparticles. Environ. Toxicol. Chem. 25 (4), 1132–1137.

Lovern, S.B., Strickler, J.R., Klaper, R., 2007. Behavioral and physiological changes in *Daphnia magna* when exposed to nanoparticle suspensions (titanium dioxide, Nano-C_{60}, and $C_{60}H_xC_{70}H_x$). Environ. Sci. Technol. 41 (12), 4465–4470.

Ma, H., Williams, P.L., Diamond, S.A., 2013. Ecotoxicity of manufactured ZnO nanoparticles — a review. Environ. Pollut. 172, 76–85.

Maier, T., 2005. Sunscreens-which and what for? Skin Pharmacol. Physiol. 18, 253–262.

Matranga, V., Corsi, I., 2012. Toxic effects of engineered nanoparticles in the marine environment: model organisms and molecular approaches. Mar. Environ. Res. 76, 32–40.

Mayland, A.D. (Ed.), 2006. Nanotechnology: A Research Strategy for Addressing Risk. Woodrow Wilson International Center for Scholars, Washtington, DC.

Menard, A., Drobne, D., Jemec, A., 2011. Ecotoxicity of nanosized TiO_2. Review of in vivo data. Environ. Pollut. 159 (3), 677–684.

Miao, A.J., Zhang, X.Y., Luo, Z., Chen, C.S., Chin, W.C., Santschi, P.H., et al., 2010. Zinc oxide–engineered nanoparticles: dissolution and toxicity to marine phytoplankton. Environ. Toxicol. Chem. 29 (12), 2814–2822.

Miller, R.J., Lenihan, H.S., Muller, E.B., Tseng, N., Hanna, S.K., Keller, A.A., 2010. Impacts of metal oxide nanoparticles on marine phytoplankton. Environ. Sci. Technol. 44 (19), 7329–7334.

Miller, R.J., Bennett, S., Keller, A.A., Pease, S., Lenihan, H.S., 2012. TiO_2 nanoparticles are phototoxic to marine phytoplankton. PLoS One 7 (1), e30321.

Moore, M.N., 2006. Do nanoparticles present ecotoxicological risks for the health of the aquatic environment? Environ. Int. 32 (8), 967–976.

Navarro, E., Baun, A., Behra, R., Hartmann, N., Filser, J., Miao, A.J., et al., 2008a. Environmental behavior and ecotoxicity of engineered nanoparticles to algae, plants, and fungi. Ecotoxicology 17 (5), 372–386.

Navarro, E., Piccapietra, F., Wagner, B., Marconi, F., Kaegi, R., Odzak, N., et al., 2008b. Toxicity of silver nanoparticles to *Chlamydomonas reinhardtii*. Environ. Sci. Technol. 42 (23), 8959–8964.

OECD, 2011. Test No. 201: Freshwater Alga and Cyanobacteria, Growth Inhibition Test. OECD Publishing.

Ovečka, M., Lang, I., Baluška, F., Ismail, A., Illeš, P., Lichtscheidl, I.K., 2005. Endocytosis and vesicle trafficking during tip growth of root hairs. Protoplasma 226 (1), 39–54.

Pettibone, J.M., Cwiertny, D.M., Scherer, M., Grassian, V.H., 2008. Adsorption of organic acids on TiO_2 nanoparticles: effects of pH, nanoparticle size, and nanoparticle aggregation. Langmuir 24 (13), 6659–6667.

Phenrat, T., Saleh, N., Sirk, K., Tilton, R.D., Lowrey, G.V., 2007. Aggregation and sedimentation of aqueous nanoscale zerovalent iron dispersions. Environ. Sci. Technol. 41 (1), 284–290.

Queiroz, A.M., Mezacasa, A.V., Graciano, D.E., Falco, W.F., M'Peko, J.C., Guimarães, F.E.G., et al., 2016. Quenching of chlorophyll fluorescence induced by silver nanoparticles. Spectrochim. Acta A 168, 73–77.

Rothen-Rutishauser, B.M., Schurch, S., Haenni, B., Kapp, N., Gehr, P., 2006. Interaction of fine particles and nanoparticles with red blood cells visualized with advanced microscopic techniques. Environ. Sci. Technol. 40 (14), 4353–4359.

Stumm, W., Morgan, J.J., 1981. Aquatic Chemistry: An Introduction Emphasizing Chemical Equilibria in Natural Waters. John Willey & Sons Inc., New Jersey.